Cancer Cell
Article

The Hippo Transducer YAP1 Transforms Activated Satellite Cells and Is a Potent Effector of Embryonal Rhabdomyosarcoma Formation

Annie M. Tremblay,[1,2,3] Edoardo Missiaglia,[4,5] Giorgio G. Galli,[1,2,3] Simone Hettmer,[2,3,9,10,11] Roby Urcia,[7] Matteo Carrara,[14] Robert N. Judson,[7,15] Khin Thway,[5,6] Gema Nadal,[7] Joanna L. Selfe,[5] Graeme Murray,[8] Raffaele A. Calogero,[14] Cosimo De Bari,[8] Peter S. Zammit,[12] Mauro Delorenzi,[4,13] Amy J. Wagers,[2,3,9] Janet Shipley,[5] Henning Wackerhage,[7] and Fernando D. Camargo[1,2,3,*]

[1]Stem Cell Program, Boston Children's Hospital, Boston, MA 02115, USA
[2]Department of Stem Cell and Regenerative Biology, Harvard University, Cambridge, MA 02138, USA
[3]Harvard Stem Cell Institute, Cambridge, MA 02138, USA
[4]SIB Swiss Institute of Bioinformatics, 1015 Lausanne, Switzerland
[5]Sarcoma Molecular Pathology Team, Divisions of Molecular Pathology and Cancer Therapeutics, The Institute of Cancer Research, Sutton, Surrey SM2 5NG, UK
[6]Department of Histopathology, Royal Marsden NHS Foundation Trust, London SW3 6JJ, UK
[7]School of Medical Sciences, University of Aberdeen, Aberdeen, AB25 2ZD Scotland, UK
[8]School of Medicine and Dentistry, University of Aberdeen, Aberdeen AB25 2ZD, Scotland, UK
[9]Howard Hughes Medical Institute and Joslin Diabetes Center, Boston, MA 02115, USA
[10]Department of Pediatric Oncology, Dana Farber Cancer Institute, Boston, MA 02115, USA
[11]Division of Pediatric Hematology/Oncology, Children's Hospital, Boston, MA 02115, USA
[12]Randall Division of Cell and Molecular Biophysics, King's College London, New Hunt's House, Guy's Campus, London SE1 1UL, UK
[13]Ludwig Center for Cancer Research and Oncology Department, University of Lausanne, 1015 Lausanne, Switzerland
[14]Molecular Biotechnology Center, Department of Biotechnology and Health Sciences, University of Torino, 10126 Torino, Italy
[15]Biomedical Research Centre, Department of Medical Genetics, University of British Columbia, Vancouver BC V6T 1Z3, Canada
*Correspondence: fernando.camargo@childrens.harvard.edu
http://dx.doi.org/10.1016/j.ccr.2014.05.029

SUMMARY

The role of the Hippo pathway effector YAP1 in soft tissue sarcomas is poorly defined. Here we report that YAP1 activity is elevated in human embryonal rhabdomyosarcoma (ERMS). In mice, sustained YAP1 hyperactivity in activated, but not quiescent, satellite cells induces ERMS with high penetrance and short latency. Via its transcriptional program with TEAD1, YAP1 directly regulates several major hallmarks of ERMS. YAP1-TEAD1 upregulate pro-proliferative and oncogenic genes and maintain the ERMS differentiation block by interfering with MYOD1 and MEF2 pro-differentiation activities. Normalization of YAP1 expression reduces tumor burden in human ERMS xenografts and allows YAP1-driven ERMS to differentiate in situ. Collectively, our results identify YAP1 as a potent ERMS oncogenic driver and a promising target for differentiation therapy.

INTRODUCTION

Rhabdomyosarcoma (RMS), the most common soft tissue sarcoma in children and adolescents, is subdivided into embryonal RMS (ERMS; ≈60%), alveolar RMS (ARMS; ≈20%), and other (≈20%) subtypes (Belyea et al., 2012). Most ARMS cases (≈80%) are associated with the presence of a PAX3/7-FOXO1A fusion gene (ARMSp), which predicts clinical outcome (Missiaglia et al., 2012) and is sufficient to cause ARMS at low frequency in mice (Keller et al., 2004). However, ≈20%

Significance

The molecular and cellular origins of ERMS are incompletely understood, and only a few ERMS-causing pathways have been identified in association with familial syndromes. Current therapies for RMS are aggressive, highly cytotoxic, and lead to life-altering sequelae for survivors. Over the past 30 years, little progress has been made in identifying more efficient and less aggressive regimens, which highlights the need for improved therapeutic approaches and a better understanding of the molecular changes underlying RMS formation and propagation. Here we identify YAP1 hyperactivity as a major molecular cause of ERMS, providing a rationale and mouse models for preclinical studies aimed at assessing the efficiency of YAP1 inhibition in combination with other regimens for differentiation therapy of ERMS.

of histologically diagnosed ARMS cases are negative for the expression of PAX3/7-FOXO1A fusion genes (ARMSn) and are indistinguishable from ERMS at the molecular level (Williamson et al., 2010). In contrast to ARMS, the oncogenic drivers in ERMS and ARMSn are still incompletely defined. A hallmark of ERMS (and other RMS subtypes) is that the cells are locked in a proliferating myoblast state despite the expression of myogenic differentiation-regulating factors such as MYOD1 and Myogenin (Saab et al., 2011). While the precise mechanism of differentiation inhibition is uncertain, it is believed that the relative abundance of MYOD1 activating or inhibiting E-protein heterodimer partners in RMS is shifted toward repressive heterodimers (Yang et al., 2009). Overcoming the terminal differentiation block in RMS would open the door for differentiation therapy, which aims to halt tumor progression by forcing the cells to differentiate into nondividing muscle fibers (Al-Tahan et al., 2012; Saab et al., 2011). However, our understanding of the mechanisms underlying this differentiation block in RMS remains insufficient to achieve better treatments.

The core Hippo pathway is regulated by many upstream signal transduction proteins in response to cues from the cellular microenvironment (Yu and Guan, 2013). It generally functions to limit organ growth and tumorigenesis by inducing the cytosolic localization of the transcriptional cofactor YAP1, especially but not solely through Ser127 phosphorylation (Zhao et al., 2007). Nuclear YAP1 promotes proliferation and inhibits apoptosis primarily by coactivating the TEAD family of transcription factors (Tremblay and Camargo, 2012). Consistent with this, the constitutively active YAP1 S127A mutant is mostly nuclear (Zhao et al., 2007) and, with the exception of the intestine (Barry et al., 2013; Zhou et al., 2011), promotes proliferation, expands undifferentiated stem cells and progenitors, and leads to tumor formation in epithelial tissues (Camargo et al., 2007; Dong et al., 2007; Schlegelmilch et al., 2011). However, the role of YAP1 in soft tissue sarcomas is still poorly defined. In C2C12 myoblasts and cultured activated satellite cells (Judson et al., 2012; Watt et al., 2010), YAP1 S127A drives proliferation and inhibits differentiation. Given that a pro-proliferation, antidifferentiation myoblast phenotype is the hallmark of RMS, here we tested whether YAP1 was involved in the development of rhabdomyosarcoma.

RESULTS

Increased YAP1 Copy Number and Elevated Expression in Human ERMS

To explore the role of YAP1 in human RMS, we first assessed the abundance and cellular localization of YAP1 protein in 78 ARMS and 196 ERMS samples. Representative YAP1 immunostainings are shown for human ERMS and ARMS tumors of each intensity category (Figure 1A). ERMS tumors expressed a significantly higher level of YAP1 protein than ARMS (Figure 1B) ($p = 0.0046$, Mann-Whitney U test). ARMS cases displayed a higher proportion of predominantly cytoplasmic staining (C), while ERMS cases displayed a greater proportion of nuclear (N) and dual nuclear/cytoplasmic staining (N/C). Indeed, there was a significant tendency for N/C expression to have a strong intensity score (chi-square test for trend, $p = 0.0002$), and YAP1 was more nuclear (N and N/C) in ERMS than ARMS (Figure 1C) (chi-square test, $p < 0.0001$, $n = 227$). We also found an association between the proliferation marker Ki67 and YAP1 staining within the ERMS subgroup, but not the ARMS (Figure 1D) (chi-square test for trend, $p = 0.079$, $n = 184$). Array CGH analysis from 79 human RMS samples (Williamson et al., 2010) revealed a significant increase in *YAP1* locus copy number in ERMS and in fusion-negative RMS, which includes ERMS and fusion-negative ARMS (ARMSn), but not in fusion-positive ARMS (ARMSp) (Figure 1E) (Fisher's exact test, $p = 0.012$). These data demonstrate a higher YAP1 expression and activity in a high proportion of ERMS cases, but not ARMS, suggesting a causative role for YAP1 in ERMS development and/or propagation.

Expression of Activated YAP1 in Mouse Skeletal Muscle Causes ERMS

To test for a causal role of high YAP1 activity in RMS, we generated doxycycline-inducible (DOX-inducible) Myf5-hYAP1 S127A mice (Figure 2A), in which DOX administration in adult mice induces the overexpression of the TetO-hYAP1 S127A transgene in the mature skeletal musculature, as well as in adult quiescent and activated satellite cells and their myoblast progeny (Beauchamp et al., 2000; Cornelison and Wold, 1997; Kuang et al., 2007; Tajbakhsh et al., 1996). After 4–8 weeks of DOX administration, adult Myf5-hYAP1 S127A mice developed a rapidly progressing and severe gait defect with marked loss of limb flexibility (Figures S1A and S1B available online), which did not allow obvious tumors to form before euthanasia was required. Hematoxylin and eosin staining (H&E) revealed extensive muscle damage, loss of mature myofibers, and the presence of newly formed fibers with centrally located nuclei, indicative of ongoing muscle regeneration (Figures 2B and 2C, arrowheads) (Judson et al., 2013). Additionally, a massive expansion of mononucleated cells was detected in the interstitial compartment of all muscles analyzed, including the tibialis anterior (TA) (Figure 2B), abdominal (Figure 2C), and gastrocnemius (GAS) muscles (Figure 2D).

Small well-demarcated tumor nodules located in the crural and/or hamstring muscles were macroscopically apparent at necropsy (Figures 2E and 2F). These tumors expressed high levels of YAP1 (Figure 2G), Desmin (Figure 2H), Myogenin (Figure 2I), and Caveolin-1 (Figure 2J) (Rossi et al., 2011). Pathologists identified the interstitial expansion and primary tumors as non-alveolar RMS histologically similar to human embryonal RMS (ERMS) of the spindle cell variant accompanied by focal pleomorphic features. The brown fat pads, also derived from the MYF5 lineage (Seale et al., 2008), appeared normal with no apparent myogenic differentiation or neoplastic lesions (Figures S1C and S1D). Dissociated cells (1×10^6) from the expanded interstitial compartment of DOX-induced Myf5-hYAP1 S127A mice produced tumors in nonobese diabetic/severe combined immunodeficient (NOD/SCID) mice with a latency ranging from 36 to 54 days (Figure S1E). These also resembled human ERMS (Figure S1F), expressed high levels of YAP1 (Figure S1G), Desmin (Figure S1H), and Myogenin (Figure S1I) and were transplantable (Figure S1J). Indeed, serial dilutions propagated the same type of secondary tumors with strikingly short latency and 100% penetrance after transplanting as few as 100 cells (Figure S1K).

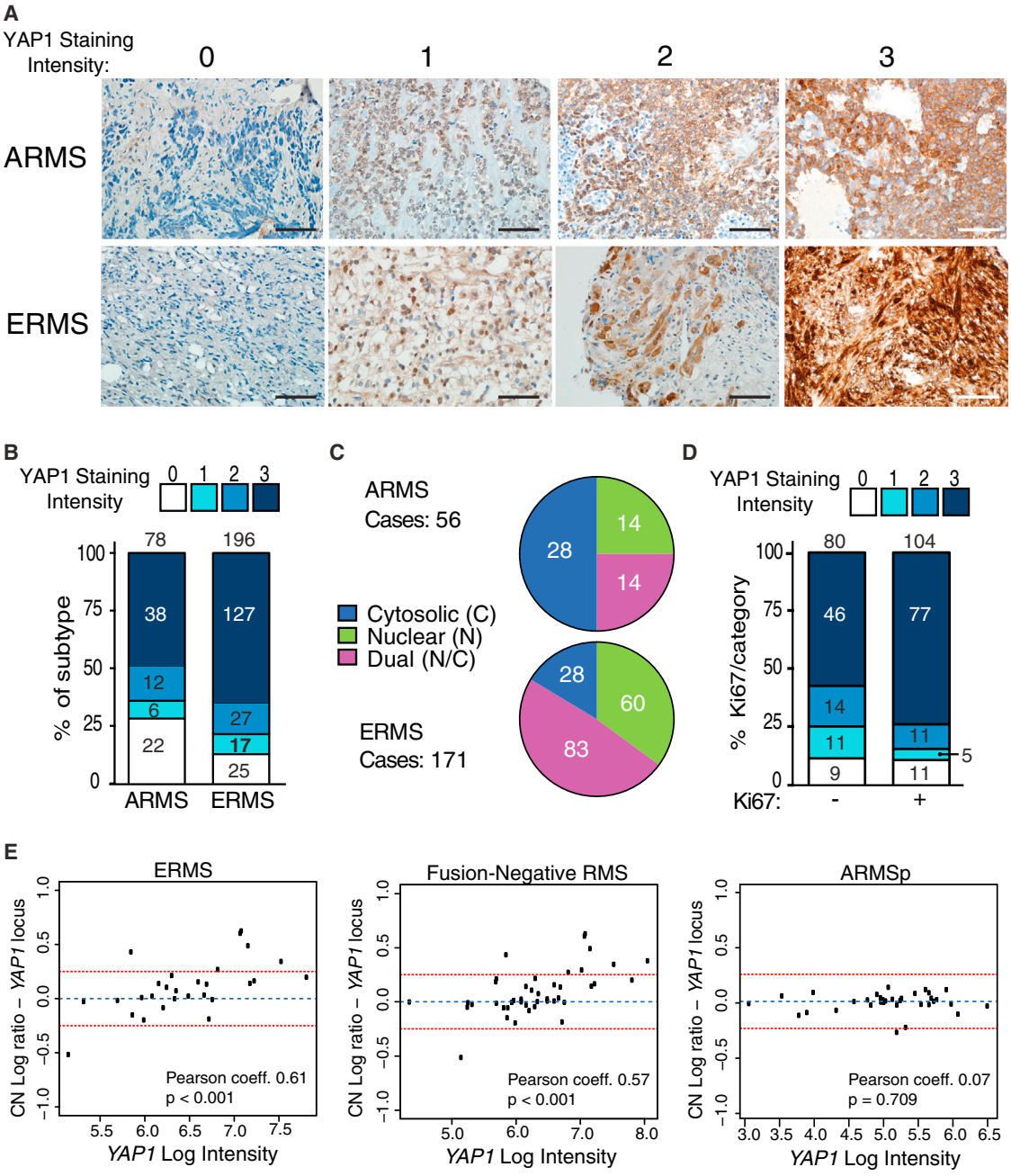

Figure 1. YAP1 Is Expressed at Higher Levels and Trends with Increased Proliferation Index in Human ERMS

(A) Immunostaining for YAP1 in human RMS samples classified by intensity level and subtype. Scale bars, 50 μm.

(B) Distribution of cases in each subtype according to YAP1 staining intensity. The number of cases is indicated on the bars.

(C) Distribution of cases according to YAP1 localization in each subtype. The number of cases is indicated on the charts.

(D) Distribution of Ki67$^-$ and Ki67$^+$ cases in ERMS according to YAP1 staining intensity. The number of cases is indicated on the bars.

(E) Plot of the log intensity expression level and local segmented copy number for *YAP1* locus in ERMS, ARMSn (fusion-negative), and ARMSp (fusion-positive) tumors. The gain and losses in each subtype were categorized based on a segmented ratio above 0.25 and below −0.25, respectively (Fisher's exact test p = 0.012).

High YAP1 Activity in the MYOD1 Lineage Induces ERMS

To confirm that RMS can arise as a result of persistent YAP1 hyperactivity in activated satellite cells or myoblasts, we additionally generated Myod1-hYAP1 S127A mice (Figure 2K) (Kanisicak et al., 2009). Within 4 weeks of DOX treatment, Myod1-hYAP1 S127A mice developed a gait phenotype similar to Myf5-hYAP1 S127A mice, with obvious primary tumors in the limbs (Figures S1L and S1M) and in abdominal muscles at

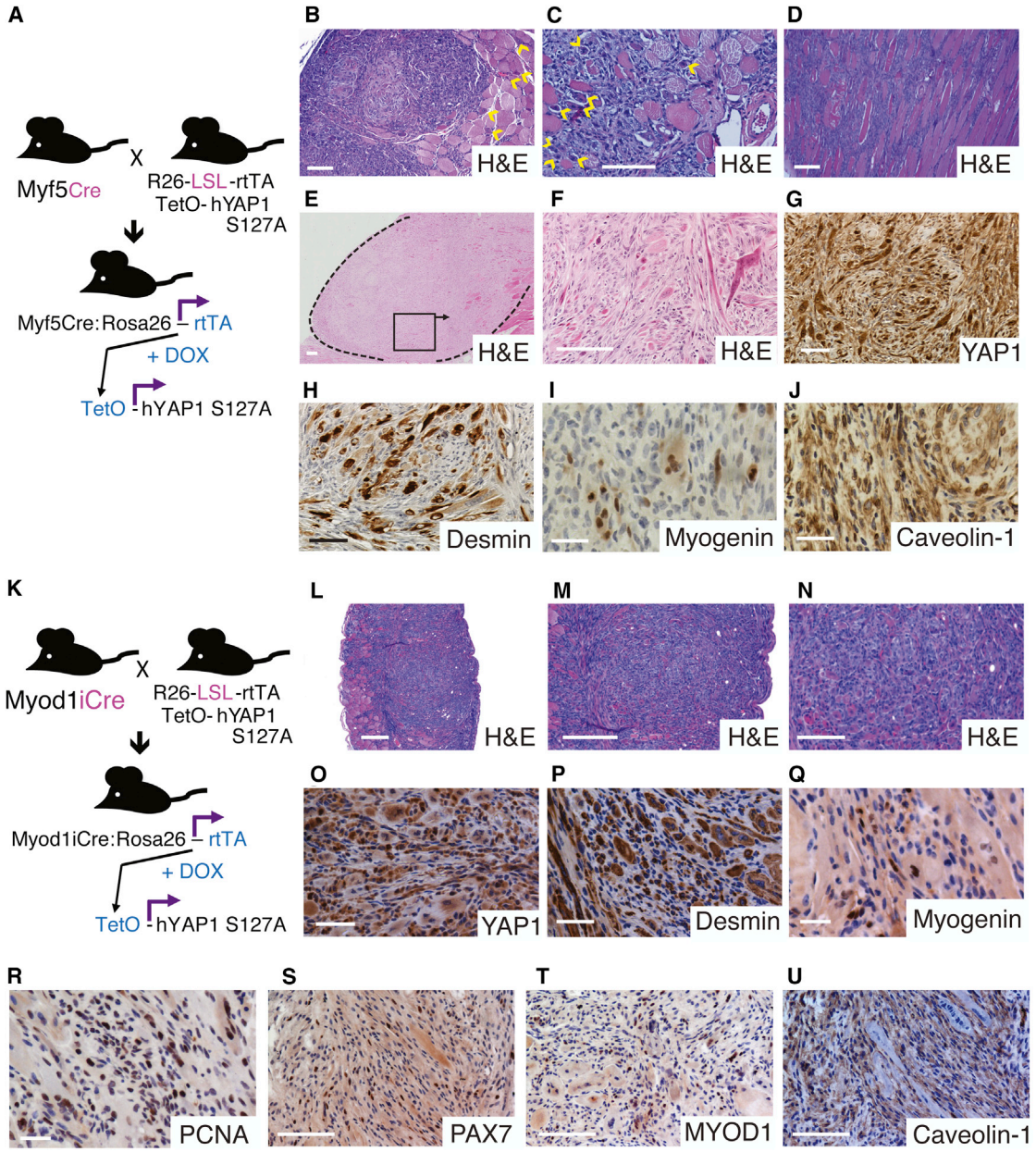

Figure 2. High YAP1 Activity in the MYF5 and MYOD1 Lineages Induces Non-Alveolar Rhabdomyosarcoma

(A) Mating strategy and alleles of the Myf5-hYAP1 S127A mice.

(B–D) Cross-section of the TA (B), abdominal wall (C), and gastrocnemius (D) of Myf5-hYAP1 S127A mice induced for 8 weeks, stained by H&E. Yellow arrowheads mark centrally located nuclei. Scale bars, 100 μm.

(E and F) Cross-section of hamstring with primary tumor outlined by dashed line (E) and at higher magnification (F) from Myf5-hYAP1 S127A mice induced for 8 weeks (n = 3). Scale bars, 100 μm.

(G–J) As in (F), immunostained for YAP1 (G), Desmin (H), Myogenin (I), and Caveolin-1 (J) (n = 3). Scale bars, 100 μm.

(K) Mating strategy and alleles of the Myod1-hYAP1 S127A mice (n = 5).

(L–N) Cross-sections of the abdominal wall of Myod1-hYAP1 S127A mice induced for 4 weeks, stained by H&E, and shown at 4X (L), 10X (M), and 20X (N) magnification. Scale bars, 200 μm (L and M). Scale bar, 50 μm (N).

(O–Q) As in (N), immunostained for YAP1 (O), Desmin (P), and Myogenin (Q). Scale bars, 50 μm.

(R–U) Sections of primary tumors from Myod1-hYAP1 S127A mice induced for 4 weeks, immunostained for PCNA (R), PAX7 (S), MYOD1 (T), and Caveolin1 (U). Scale bars, 50 μm (R), and 100 μm (S–U).

See also Figure S1.

necropsy. H&E revealed signs of muscle damage, myofiber regeneration, and importantly, a widespread amplification of mononucleated cells in the interstitial compartment of the TA (Figures S1N and S1O) and abdominal muscles (Figures 2L–2N), along with the presence of centrally located nuclei in the remaining fibers (Figure S1O, arrowheads). As in Myf5-hYAP1 S127A mice, cells in the amplified interstitial compartment expressed YAP1 (Figure 2O), Desmin (Figure 2P), and Myogenin (Figure 2Q). In addition, PCNA (Figure 2R), PAX7 (Figure 2S), MYOD1 (Figure 2T), and Caveolin-1 (Figure 2U) expression suggested extensive proliferation and a low degree of myogenic differentiation, compatible with an expansion of activated satellite cells and/or myoblasts. Dissociated primary tumor cells (0.5×10^6) propagated tumors in NOD/SCID (Figure S1P) with a similar histology as the secondary tumors from the Myf5-hYAP1 S127A model (Figure S1Q) and similar expression of YAP1 (Figure S1R), Desmin (Figure S1S), and Myogenin (Figure S1T). Collectively, these results reveal that $MYF5^+$ and $MYOD1^+$ activated satellite cells or myoblasts can be the cells of origin of YAP1-ERMS, which is further supported by the enhanced soft agar colony-forming potential of C2C12 myoblasts expressing hYAP1 S127A (Figure S1U).

High YAP1 Activity Does Not Induce Satellite Cells Activation but Transforms Activated Satellite Cells

Next we addressed the question of whether persistent YAP1 hyperactivity is sufficient to both activate and transform satellite cells. To overexpress hYAP1 S127A in quiescent and activated satellite cells, we generated DOX-inducible Pax7-hYAP1 S127A mice (Figure 3A) (Lepper and Fan, 2010). DOX was given for 8 weeks, and muscle injury was induced via cardiotoxin (CTX) injection to the right hindlimb 3 weeks after the hYAP1 S127A induction in $PAX7^+$ cells (Figure 3B). Surprisingly, the muscle morphology in the uninjured left hindlimb was unaffected after 8 weeks of DOX, and H&E staining showed no signs of expansion of the interstitial compartment (Figure 3C). Likewise, the percentage of satellite cells, assessed by the ratio of $PAX7^+$ nuclei/total nuclei, remained unchanged (Figures S2A and S2B). In contrast, the injured muscles of Pax7-hYAP1 S127A overexpressing mice displayed massive amplification of mononucleated cells 5 weeks after injury (Figure 3D), which was histologically consistent with RMS as determined by pathological examination. The core of the injured muscle expressed high levels of YAP1 (Figure S2C), PCNA (Figure S2D), Desmin (Figure S2E), and Myogenin (Figure S2F) with a low level of PAX7 expression (Figure S2G). We additionally introduced a ZsGreen1 reporter allele in Pax7-hYAP1 S127A mice in order to track the activated progeny of quiescent $PAX7^+$ cells after CTX injury (Figure 3E). A longer DOX induction period after injury led to the development of $ZsGreen1^+$ primary tumors at the injury site by using either CTX or a barium chloride injury method (Figure 3F). Sorted $ZsGreen1^+$ cells from those primary tumors produced secondary $ZsGreen1^+$ tumors expressing high levels of YAP1 (Figure 3G), Desmin (Figure 3H), and MYOD1 (Figure 3I), while PAX7 expression was overall low (Figure 3J shows a representative patch of $PAX7^+$ cells). Human ERMS tumors notably express PAX7 at variable levels (Tiffin et al., 2003), and while viewed as indicative of a satellite cell origin, PAX7 expression is not a diagnostic criteria for RMS classification. Collectively, our results on three transgenic mouse models (*Myf5*-, *Myod1*-, and *Pax7*-driven hYAP1 S127A expression) and two types of injury strongly suggest that persistent hyperactivity of YAP1 in activated but not quiescent satellite cells can potently cause ERMS-like tumors with remarkably short latency in mice.

Normalization of YAP1 Activity in YAP1-Driven ERMS Releases the YAP1-Imposed Differentiation Block In Situ

To test whether YAP1 reduction causes tumor regression, we withdrew DOX from host mice bearing secondary tumors following transplantation of sorted $ZsGreen1^+$ Pax7-hYAP1 S127A primary tumor cells from the injury site (Figure 4A, top panel). DOX-withdrawn tumors regressed to ≈ 50% of their original size in 10 days (Figure 4A, bottom panel) and coexpressed the myogenic differentiation marker sarcomeric myosin heavy chain (MyHC) and ZsGreen1 in myofibers at their core (Figure 4B). We observed a similar regression in Myf5-hYAP1 S127A allograft tumors 12 days after DOX withdrawal (Figure 4C). These tumors, after 6 days OFF DOX (OFF6) (Figure 4D), showed a marked decrease in the expression of YAP1 (Figure 4E), PCNA (Figure 4F), and Caveolin-1 (Figure 4G). Expression of Myogenin (Figure 4H) appeared unchanged, while Desmin immunostaining was suggestive of newly formed myofibers (Figure 4I). Consistently, Caveolin-3 (Figure 4J) and MyHC (Figure 4K) expression increased. Furthermore, coexpression of MyHC and ZsGreen1 (Figure 4L) at the core of the regressing tumors (Figures S3A and 3SB) confirmed the ability of the YAP1-ERMS tumor cells to differentiate into mature skeletal muscle in situ once YAP1 expression is normalized. In culture, $ZsGreen1^+$ YAP1-ERMS cells from Myf5-hYAP1 S127A secondary tumors could be expanded in the presence of DOX (Figure S3C), but did not proliferate as well in its absence (Figure S3D). These cells also formed $MyHC^+$ and $ZsGreen1^+$ double positive myotubes when plated at high density and subjected to differentiation conditions for 4 days in the absence of DOX (Figure S3E). These results suggest that persistent hYAP1 S127A hyperactivity causes ERMS-like tumors in mice both by promoting proliferation and imposing a differentiation block, which can be overcome once YAP1 activity is reduced.

Identification of YAP1 Target Genes in YAP1-ERMS

To characterize the mechanisms by which YAP1 drives ERMS, we aimed to identify the YAP1 target genes that could explain the sustained myoblast proliferation and differentiation-block phenotype of ERMS. We combined global gene expression analyses with chromatin immunoprecipitation-sequencing (ChIP-Seq) for the YAP1 cofactor TEAD1. YAP1 and TEAD1 mostly co-occupy the same promoters in MCF10A cells (>80% overlap) (Zhao et al., 2008) and directly interact in proliferating mouse myoblasts (Judson et al., 2012). YAP1 does not bind DNA directly, so interaction with TEAD factors is responsible for most, if not all, of YAP's functions in vivo (Schlegelmilch et al., 2011), and identification of YAP1 target genes is reliably associated with TEAD binding sites (Lian et al., 2010; Zhao et al., 2008).

We first used microarray analysis to identify potential YAP1 target genes in the YAP1-ERMS tumors. We reasoned that YAP1 direct target genes would show a transcriptional response to reduction of transgenic YAP1 levels in regressing YAP1-ERMS

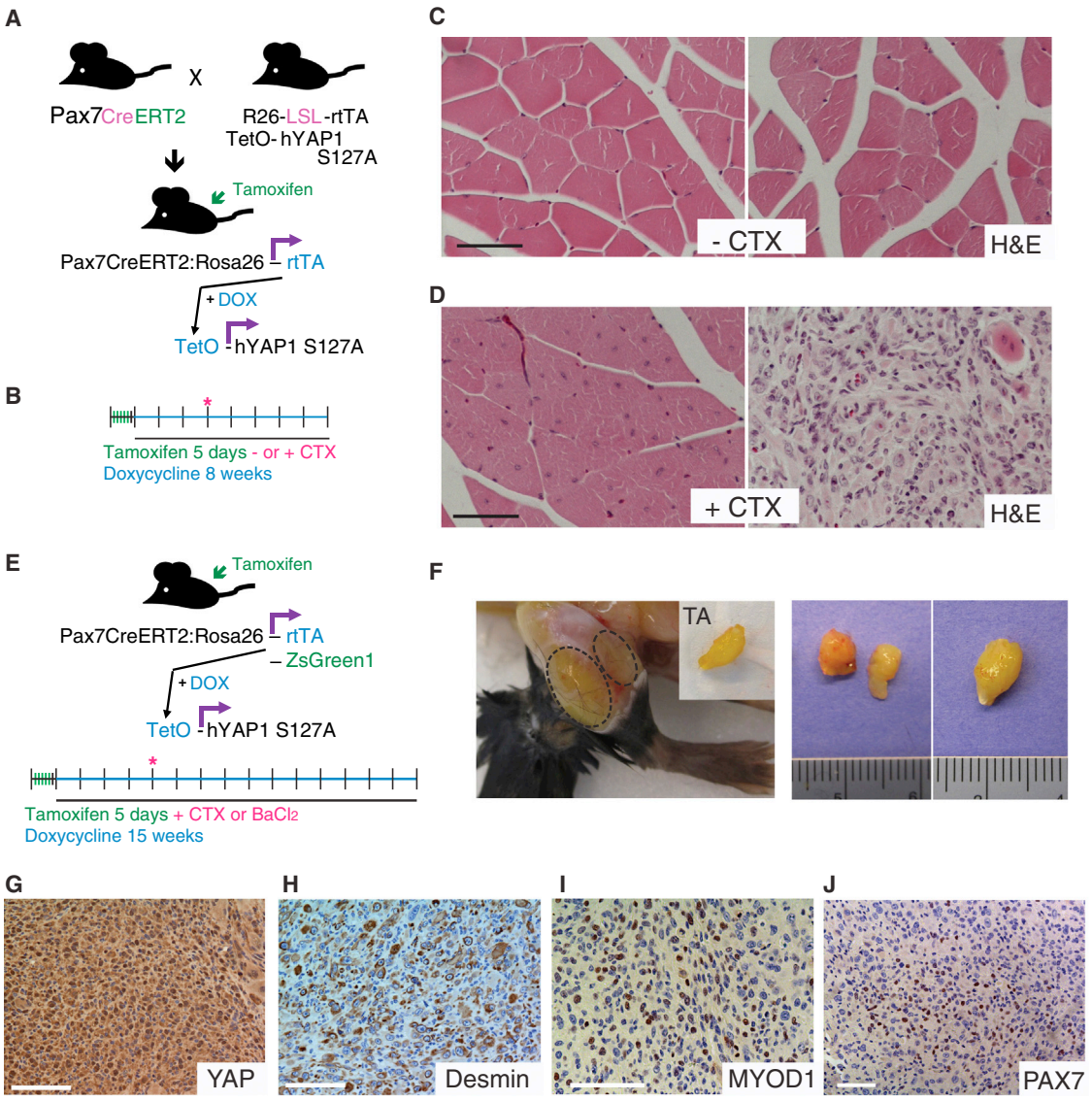

Figure 3. High YAP1 in PAX7$^+$ Satellite Cells Causes Rhabdomyosarcoma Only after Injury

(A) Mating strategy and alleles of the Pax7-hYAP1 S127A mice.

(B) Timeline of treatments.

(C) Cross-section of uninjured GAS in control (left) and Pax7-hYAP1 S127A mice (right) (n = 3).

(D) Cross-section of cardiotoxin-injured GAS in control (left) and Pax7-hYAP1 S127A mice (right) (n = 3).

(E and F) Diagram of the longer induction regimen in ZsGreen1-traced Pax7-hYAP1 S127A mice (E) and the resulting ZsGreen$^+$ primary tumors at the injury site (F) after cardiotoxin (left) or barium chloride injury (center and right). The dashed line circumscribes the tumor location (n = 3).

(G–J) Sections of Pax7-hYAP1 S127A allografts immunostained with YAP1 (G), Desmin (H), MYOD1 (I), and PAX7 (J). The representative PAX7$^+$ region is shown. All scale bars, 100 μm. See also Figure S2.

after short-term DOX withdrawal for 3 and 6 days (OFF3, OFF6) (Figure 5A). We confirmed the decreased expression of the hYAP1 transgene and the YAP1 target gene *Cyr61* by quantitative polymerase chain reaction (qPCR) (Figure S4A). The expression of satellite cell markers *Pax7* and *Myf5* also decreased in regressing tumors (Figure S4A). *Myod1* and the terminal differentiation marker myosin heavy chain, *Myh4*, were upregulated during the regression compared to day 0 tumors (Figure S4A). Hierarchical clustering of microarray profiles showed a return of regressing tumors toward terminally differentiated muscle (Figure 5B), consistent with re-expression of myogenic differentiation markers in regressing tumors (Figures 4J–4L).

We next identified differentially expressed genes between YAP1-driven ERMS and each of the three conditions of low YAP1 activity: skeletal muscle control and DOX withdrawn for 3 days and 6 days. The overlap between the 3 lists identified a subset of 633 YAP1-upregulated genes (Figure 5C), as well as 249 YAP1-downregulated genes (Figure 5D). Within each list, 71% of the genes were also associated with TEAD1 occupancy in YAP1-ERMS cells (Figure 5E and Table S1), suggesting that

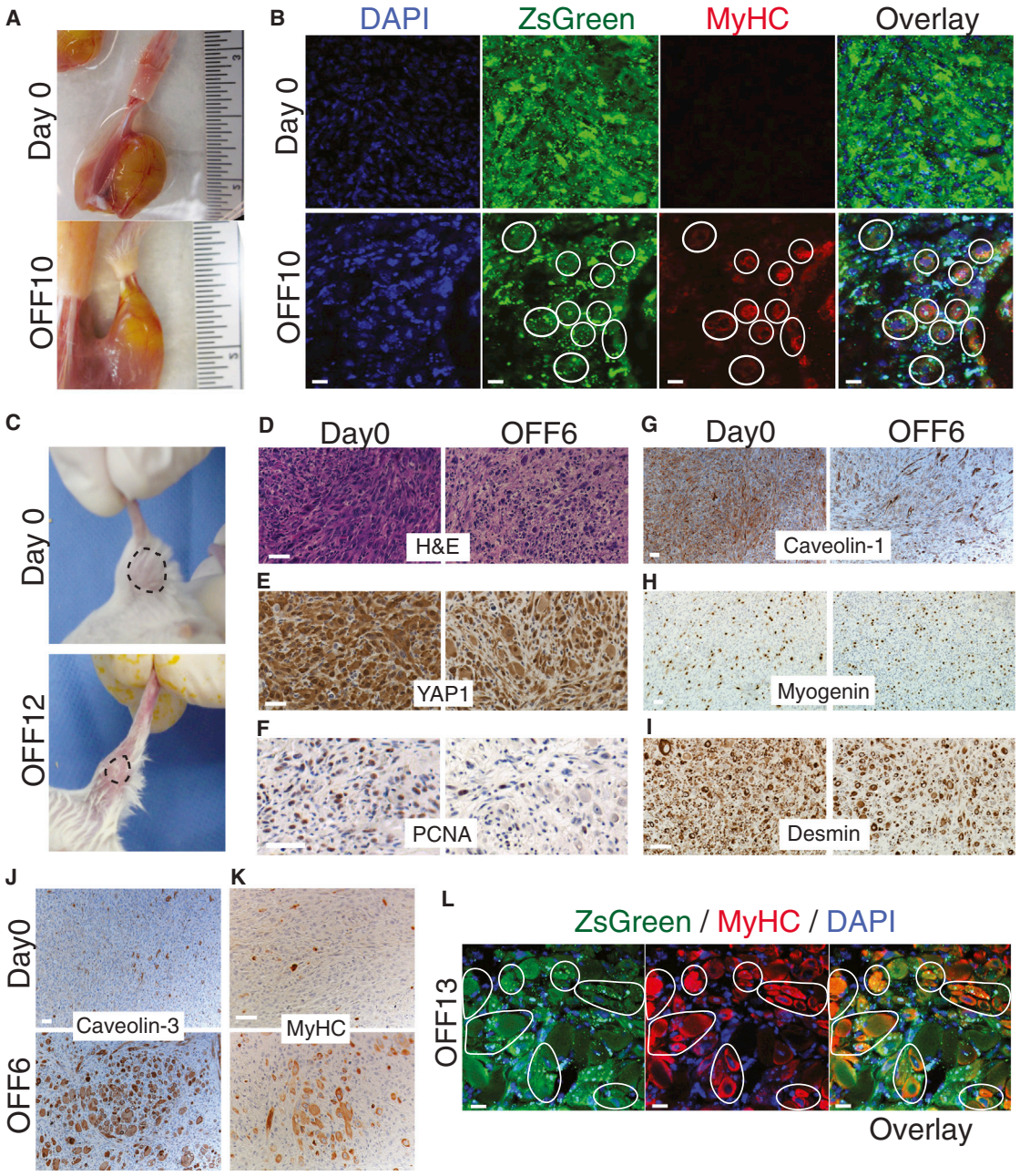

Figure 4. Normalization of YAP1 Expression Allows Differentiation of YAP1-ERMS Tumors In Situ

(A) Representative picture of Pax7-hYAP1 S127A secondary tumors in situ at day 0 (top panel) and Pax7-hYAP1 S127A secondary tumors in situ following DOX withdrawal for 10 days (bottom panel).

(B) Frozen section of tumors in (A) immunostained for MyHC (red) and DAPI (blue). ZsGreen and MyHC double positive fibers are circled.

(C) Representative picture of the Myf5-hYAP1 S127A secondary tumors in situ before and after DOX withdrawal for 12 days. The dashed line circumscribes the tumor location.

(D) H&E staining of tumor sections at day 0 and after 6 days of DOX withdrawal (OFF6).

(E–K) As in (D), immunostained for YAP1 (E), Desmin (F), Myogenin (G), PCNA (H), Caveolin-1 (I), Caveolin-3 (J), and MyHC (K).

(L) Frozen section of ZsGreen-traced tumors after 13 days of DOX withdrawal (OFF 13), immunostained for MyHC (red) and DAPI (blue). ZsGreen and MyHC double positive fibers are circled.

All scale bars, 50 μm. See also Figure S3.

most of these genes are likely direct transcriptional targets of YAP1-TEAD1. Gene ontology (GO) analysis revealed enrichment for terms related to cellular proliferation, cell cycle, and mitosis in the YAP1-ERMS-upregulated target gene list (Figure 5F). In contrast, the YAP1-ERMS-repressed target gene list was enriched for GO terms related to muscle contraction (Figure 5G)

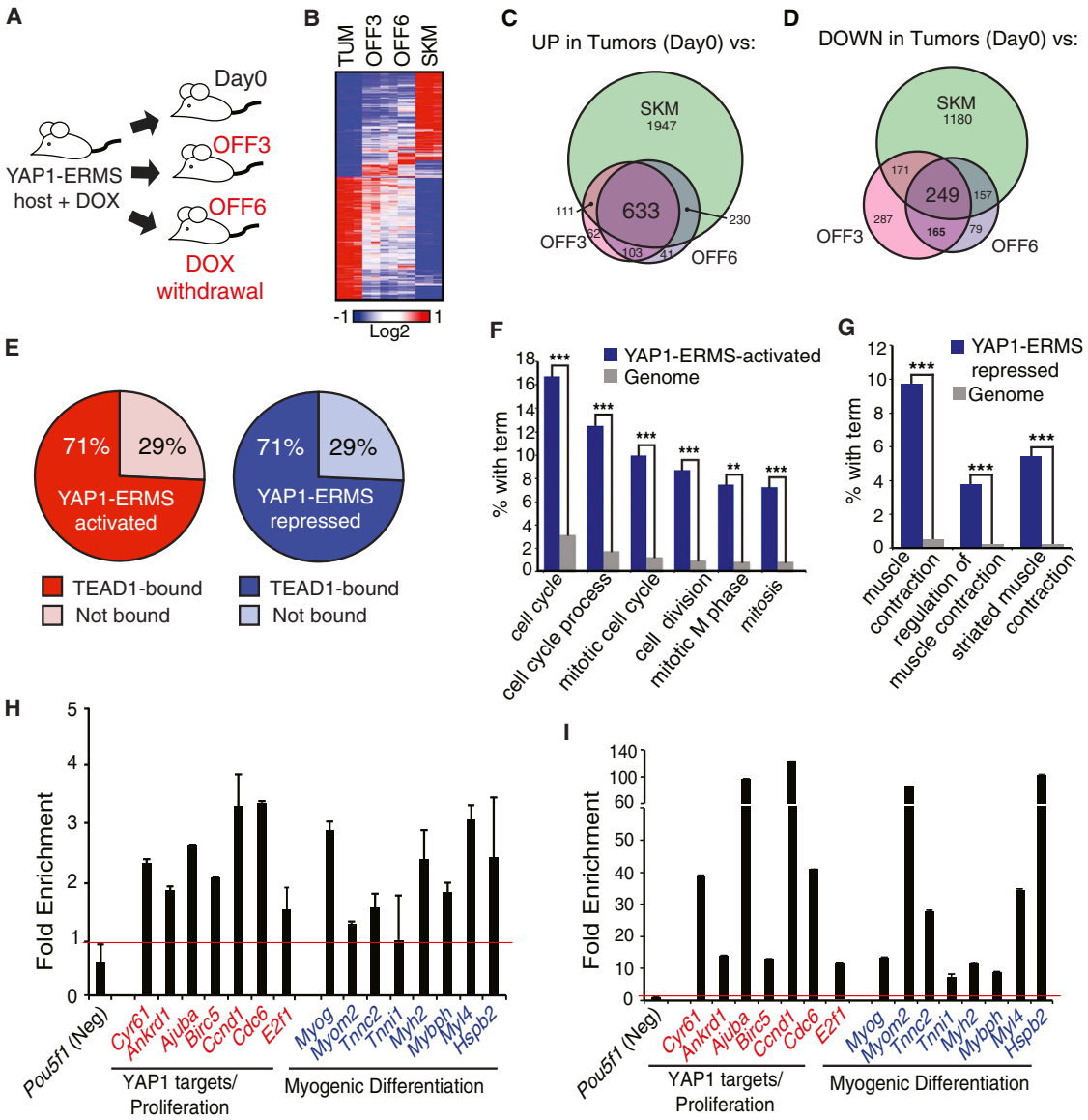

Figure 5. Combined Gene Expression Profiling and TEAD1 ChIP-Seq Analyses Identify YAP1-TEAD1 Direct Target Genes Signatures in YAP1-Driven ERMS

(A) Diagram of the tumor regression experiments used in the microarray analysis.

(B) Heat map showing hierarchical clustering of global gene expression in normal skeletal muscle (SKM), day 0 (TUM), and DOX-withdrawn (OFF3 and OFF6) tumors.

(C and D) Venn diagram showing the overlap between the genes upregulated (C) and downregulated (D) in the YAP1-ERMS tumors (TUM) versus normal skeletal muscle (SKM) and the regressed tumors at day 3 (OFF3) and 6 (OFF6).

(E) Pie charts representing the percentage of common YAP1-regulated genes (TUM versus SKM-OFF3-OFF6) bound by TEAD1.

(F and G) Gene ontology analysis of the YAP1-ERMS-activated (F) and YAP1-ERMS-repressed (G) signatures (**$p < 0.01$; ***$p < 0.001$).

(H and I) ChIP-qPCR validations of YAP1 (H) and TEAD1 (I) occupancy on selected loci associated with upregulated (red) and downregulated (blue) genes in the YAP1-ERMS microarray. Data were presented in fold enrichment over IgG ± SD.

See also Figure S4 and Table S1.

and contained mostly target genes of myogenic regulatory factors MYOD1, Myogenin, MEF2, and SRF (Figure S4B), suggesting a decreased activity of these factors when YAP1 activity is high. We next performed ChIP-qPCR validations for YAP1 (Figure 5H) and TEAD1 (Figure 5I) occupancy on a subset of peaks selected by the combination of microarray and ChIP-Seq analyses, confirming the correlation between TEAD1 binding peaks and YAP1 occupancy. Collectively, this suggests that YAP1-TEAD1 not only directly drives gene expression necessary for sustained proliferation but also contributes to blocking myogenic differentiation by repressing genes that are normally expressed in differentiated skeletal muscle.

YAP1 Is Integrated in the Myogenic Differentiation Program and Represses Terminal Differentiation Genes

Studies since the late 1980s reported occurrence of TEAD DNA binding sites, named muscle CAT (MCAT) elements, in the promoters of genes that are selectively expressed in differentiated skeletal muscle (Yoshida, 2008). Here we confirm and extend this observation genome-wide. Using motif enrichment analyses, we identified the overrepresentation of Myogenin, MEF2, or SRF consensus sequences within TEAD peaks or around the promoter of TEAD1-associated genes (Figure S5A). Nearly one-third (27%) of TEAD1 peaks in ''undifferentiated'' YAP1-ERMS cells are aligned with MYOD1, Myogenin, and/or SRF binding peaks in differentiated C2C12 myotubes (Figure S5B), suggesting that YAP1-TEAD1 globally regulates muscle lineage-specific gene expression in YAP1-ERMS. GO analysis of the shared TEAD1-MYOD1-Myogenin-SRF loci returned terms compatible with the YAP1-ERMS phenotype and with the role of YAP1 in the repression of the myogenic differentiation program (Figures S5C and S5D), while the TEAD1-only sites associated generally with immune processes and signaling pathways (Figure S5E).

Among the genes harboring adjacent binding sites for TEAD1-MYOD1-Myogenin-SRF, a large number of repressed genes were associated with terminal muscle contraction and differentiation. The expression of these genes was reduced in YAP1-driven ERMS but increased when YAP1 activity was lowered by DOX withdrawal (Figure 6A). Interestingly, MYOD1 and Myogenin binding occupancy increases during myogenic differentiation from myoblasts to myotubes, on loci shared with TEAD1 (Figure S5F). This correlates with the concomitant decrease in YAP1 activity during myogenic differentiation (Judson et al., 2012; Watt et al., 2010). We thus hypothesized that YAP1-TEAD1 occupancy could impinge on MYOD1 and MEF2 binding on shared sites associated with repressed muscle differentiation genes. To test this we evaluated the occupancy of MEF2 and MYOD1 on a selection of genes associated with myogenic differentiation or proliferation while altering the levels of YAP1 in cultured YAP1-ERMS cells via DOX withdrawal (Figure 6B). This analysis revealed that reduction of hYAP1 S127A expression, leading to differentiation of YAP1-ERMS cells, resulted in increased occupancy of MEF2 (Figure 6C) and/or MYOD1 (Figure 6D) specifically on myogenic differentiation genes, but not on proliferation-related genes. Such functional interplay between YAP1 and myogenic factors at shared loci cannot be explained by changes in MEF2 or MYOD1 expression levels as their expression did not increase during YAP1-ERMS differentiation (Figure 6E). However, both expression (Figure 6E) and occupancy of TEAD1 (Figure 6F) decreased during YAP1-ERMS cell differentiation on all genes tested, including proliferation-associated genes. Our data indicate that the sustained presence of YAP1-TEAD1 plays a role in repressing differentiation genes, partly by impinging on the differentiation promoting activities of myogenic transcription factors at muscle differentiation-associated loci.

YAP1 Upregulates Oncogenes and Inhibitors of Myogenic Regulatory Factors in Mouse YAP1-ERMS and Human ERMS Cells

Additionally, we observed upregulation of several canonical YAP1 target genes and RMS-related oncogenes (Figures 6G and S5D) in YAP1-ERMS, identifying YAP1 as a meta-oncogene and supporting the potency of YAP1 to trigger ERMS in mice. Among YAP1 upregulated genes, we identified a subset that encode known inhibitors of MYOD1 and MEF2 activity, including *Id2*, *Twist1*, *Mdfic*, *Snai1*, *Snai2*, and *Cabin1* (Figure 6G). Loci associated with the latter category of genes were also bound by YAP1 (Figure 6H) and TEAD1 (Figure 6I) in YAP1-ERMS cells and were upregulated at the protein level in induced muscle and YAP1-ERMS primary tumors from Myod1-hYAP1 S127A mice (Figure 6J). This suggests that YAP1 can block differentiation not only by affecting the occupancy of MYOD1 and MEF2 at myogenic differentiation-associated loci but also by upregulating the expression of inhibitors of myogenic transcription factors.

Interestingly, most YAP1-TEAD1 bound target genes validated in mouse YAP1-ERMS (Figures 5H, 5I, 6H, and 6I) were also bound by YAP1 (Figure S5G) and TEAD1 (Figure S5H) in human ERMS RD cells, and some of these loci were also shared by MEF2 (Figure S5I) and MYOD1 (Figure S5J). In addition, gene expression analysis of the validated YAP1-TEAD1 target genes in RD cells (Figure S5K) and human ERMS (Figure S5L) shows regulation similar to mouse YAP1-ERMS (Figures 6A and 6G), suggesting that the transcriptional program of YAP1 and its role in blocking differentiation is similar in human ERMS. Indeed, using the YAP1-ERMS signatures identified in mouse (Figure 5E and Table S1), we could assess YAP1 activity in a microarray of human fetal myoblasts undergoing differentiation. Consistent with the impeding effect of YAP1 S127A on the differentiation of mouse myoblasts in vitro (Judson et al., 2012; Watt et al., 2010), expression of *YAP1* mRNA (Figure S5M) and the YAP1-ERMS-activated signature (Figure S5N) decreased progressively when human fetal myoblasts differentiated. Concurrently, expression of the YAP1-ERMS-repressed signature increased (Figure S5O). These data validate use of the YAP1-ERMS signatures as YAP1 activity readout in human cells and suggest that a decrease in YAP1 activity is also associated with myogenic differentiation in human myoblasts, as in mouse.

These analyses in YAP1-ERMS and human RD cells demonstrate that YAP1-TEAD1 binding is associated with three categories of direct target genes. YAP1-TEAD1 binding is associated first with expression of genes that promote proliferation and/or transformation, second, with repression of genes that are normally expressed in differentiated skeletal muscle, and third, with increased expression of MYOD1 and MEF2 inhibitors. Collectively, this suggests that persistent YAP1 hyperactivity not only drives proliferation and transformation, but also represses differentiated muscle lineage-specific genes, imposing a global differentiation block, which is a hallmark of RMS.

High YAP1 Activity Associates with Higher Stage in Fusion-Negative RMS and Trends with Poorer Prognosis

We next confirmed the importance of YAP1 activity in human RMS using two large series of human RMS primary tumors totaling 235 samples. First, *YAP1* expression was higher in human ERMS and ARMSn compared to ARMSp (Figure 7A). YAP1 activity was next assessed using the YAP1-ERMS-activated and YAP1-ERMS-repressed signatures. YAP1 activity was high in all RMS subtypes compared to skeletal muscle

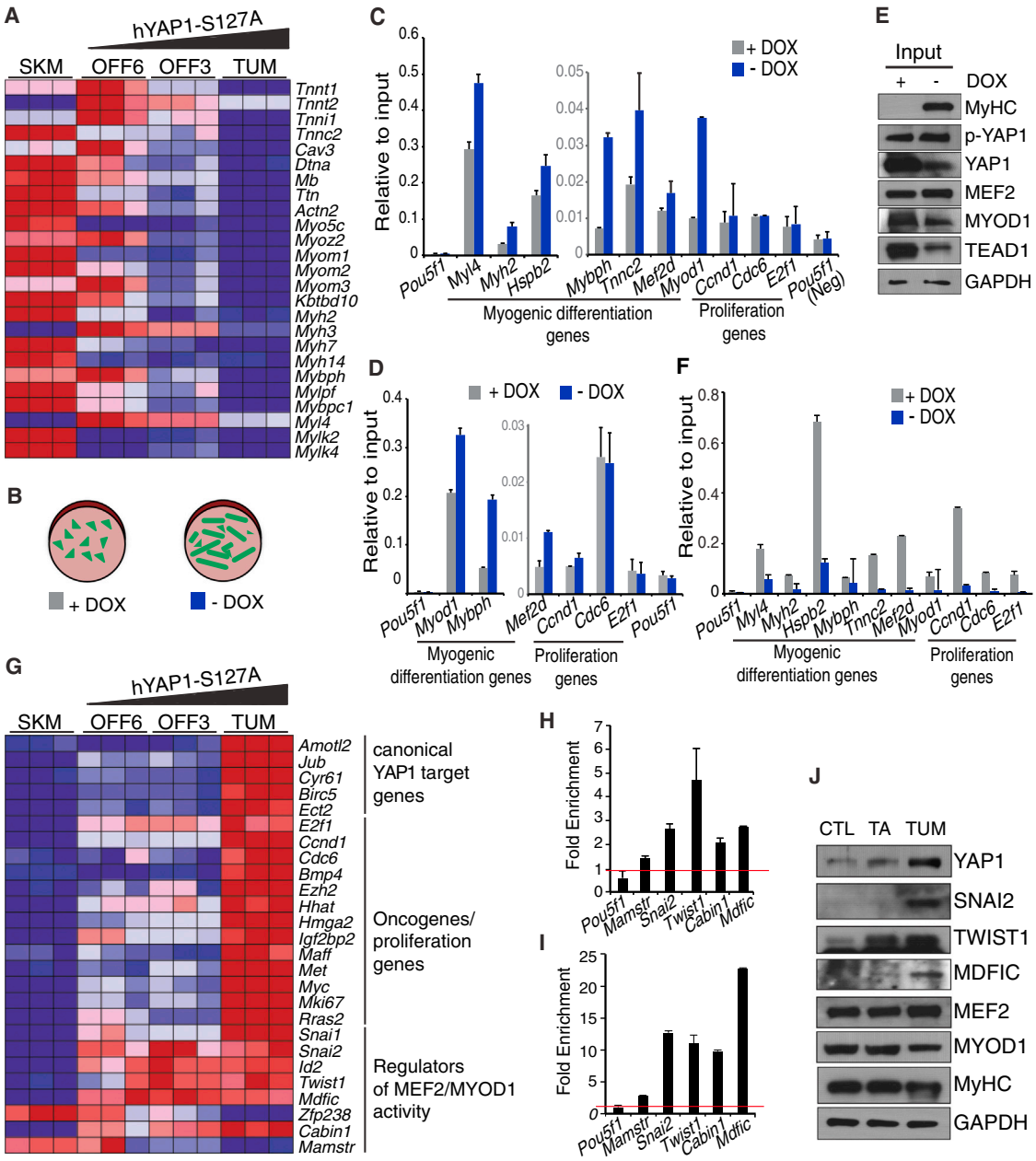

Figure 6. YAP1-TEAD1 Globally Repress MYOD1 and/or MEF2 Activity and Upregulate Oncogenes in YAP1-ERMS Cells

(A) Heat map representing the expression of terminal differentiation genes repressed by YAP1-TEAD1 in YAP1-ERMS.

(B) Culture conditions of YAP1-ERMS cells used in (C)–(F).

(C and D) ChIP-qPCR for MEF2 (C) and MYOD1 (D) in YAP1-ERMS cells in proliferation (+ DOX) and differentiation (− DOX) conditions on a subset of terminal differentiation and proliferation-associated genes. The negative region (Neg) is *Pou5f1*. Errors are ±SD. Note the difference in the y axis scales between the left and the right sides of the graphs.

(E) Protein levels of YAP1, phospho-YAP1 (p-YAP1), TEAD1, MEF2, MYOD1, and MyHC in proliferating (+ DOX) and differentiated (− DOX) YAP1-ERMS.

(F) ChIP-qPCR for TEAD1 in YAP1-ERMS cells in proliferation (+ DOX) and differentiation (− DOX) conditions on a subset of terminal differentiation and proliferation-associated genes. The negative region (Neg) is *Pou5f1*. Errors are ±SD.

(G) Heat map representing the expression of genes from three categories upregulated by YAP1-TEAD1 in YAP1-ERMS.

(H and I) ChIP-qPCR for YAP1 (H) and TEAD1 (I) on loci associated with inhibitors of MYOD1 and/or MEF2 activity. The negative site is *Pou5f1*. The fold enrichment over IgG is normalized to 1 (red line). Errors are ±SD.

(J) Western blot analysis for YAP1, MyHC, TEAD1, MEF2, and MYOD1 as well as genes involved in repression of MYOD1 activity (SNAI2, TWIST1, MDFIC) in control muscle (CTL), induced TA (TA), and primary tumors (TUM) from Myod1-hYAP1 S127A mice induced with DOX for 4 weeks.

See also Figure S5.

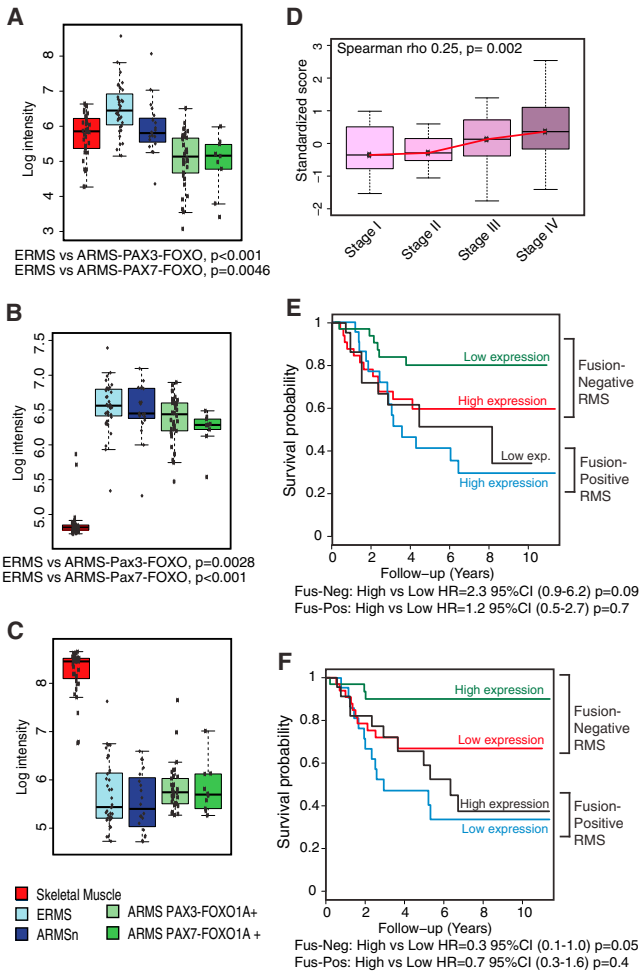

Figure 7. The YAP1-ERMS Signatures Cluster Fusion-Negative RMS Tumors According to Stage and Severity

(A–C) Expression score of *YAP1* mRNA (A), YAP1-ERMS-activated (B), and YAP1-ERMS-repressed signature (C) scores in in human RMS tumors in the ITCC/CIT data set. Differences were tested by Wilcoxon signed-rank test.

(D) Box plot showing the association between the YAP1-ERMS-activated signature and tumor stage in fusion-negative RMS cases (Spearman rho 0.25, p = 0.002).

(E and F) Kaplan-Meier curves of survival in cases of fusion-negative and fusion-positive RMS with high and low expression scores of the YAP1-ERMS-activated (G) and YAP1-ERMS-repressed (H) signatures.

See also Figure S6 and Tables S2 and S3. All whisker bars represent 1.5 times the interquartile range (1.5 IQR), and the central lines represent the median value.

control, but also significantly elevated in ERMS and ARMSn over ARMSp (Figure 7B), while the expression of the YAP1-ERMS-repressed signature was low in all subtypes (Figure 7C). The YAP1-ERMS-activated signature was significantly enriched in all RMS subtypes considered together versus skeletal muscle, along with the gene expression signatures of embryonic stem cells, Notch, and satellite cells activation (Figure S6A and Table S2). Remarkably, the YAP1-ERMS-activated signature was enriched specifically in ERMS versus ARMSp (Figure S6B), and more significantly than the satellite cells activation signature, which was previously reported as a hallmark of ERMS (Hatley et al., 2012; Rubin et al., 2011). These results show that YAP1 activity is elevated in human ERMS and suggest that our YAP1-ERMS signatures could constitute a useful indicator of YAP1 activity in human RMS tumors as well.

We then investigated whether YAP1 activity is associated with prognosis and/or outcome in human RMS. Indeed, stage 3 and 4 tumors were significantly positively associated with higher YAP1 activity based on a multivariable linear regression model including clinicopathological features linked to RMS outcome (Missiaglia et al., 2012) (Table S3 and Figure 7D), such as tumor histology, age, and tumor location. We next defined HIGH expression and LOW expression subgroups for both YAP1-ERMS signatures (activated and repressed) within each RMS subtypes and identified a trend (log rank test, p = 0.09) toward a poorer outcome for the subgroup with a higher expression score of the YAP1-ERMS-activated signature in fusion-negative, but not in fusion-positive, tumors (Figure 7E). Consistently, the reverse analysis using the YAP1-ERMS-repressed signature showed that the low expression subgroup associated with poorer outcome (log rank test, p = 0.05) in fusion-negative tumors, but not in fusion-positive tumors (Figure 7F). Taken together, these results suggest that the YAP1-ERMS signatures can better segregate the fusion-negative RMS subtypes in terms of stage and outcome, possibly identifying tumors with higher proliferation rates and lower differentiation levels.

YAP1 Knockdown Decreases Proliferation and Tumorigenicity while Increasing Differentiation Capacity of Human ERMS

We next hypothesized that lowering YAP1 in human ERMS would release the terminal differentiation block. We stably introduced a DOX-inducible hYAP1 knockdown construct in RD cells (RD-TetO-shYAP1). DOX treatment of RD-TetO-shYAP1 cells for 5 days induced a marked reduction of YAP1 protein (Figure 8A) and mRNA levels (Figure 8B). Expression of the proliferation marker *E2F1* (Figure 8B) and EdU incorporation also decreased (Figure 8C), while the number of MyHC$^+$ cells per myotubes increased, demonstrating an enhanced myogenic differentiation (Figure 8D). DOX-treated RD-TetO-shYAP1 cells cultured in soft agar formed fewer and smaller colonies (Figures 8E and 8F), suggesting that YAP1 knockdown additionally decreases tumorigenicity in vitro.

To assess the effects of YAP1 knockdown on ERMS tumorigenicity in vivo, we transplanted either control or hYAP1 knockdown RD cells into the gastrocnemius muscle of NOD/SCID mice. Orthotopic xenografts from the hYAP1 knockdown RD cells were 42% smaller than tumors originating from control cells (Figure 8G). Efficient knockdown of YAP1 protein in the DOX-treated xenografts was confirmed by immunostaining for YAP1 (Figure 8H), which also correlated with decreased expression of human Ki67 (Figure 8I) and increased expression of MyHC (Figures 8J and 8K), indicating a greater degree of differentiation of tumors in the YAP1 knockdown condition. These results show that the tumorigenicity and low differentiation potential of ERMS can be rescued in vitro and in vivo by decreasing YAP1 expression, which functionally validates the potential benefits of YAP1 inhibition for differentiation therapy of ERMS.

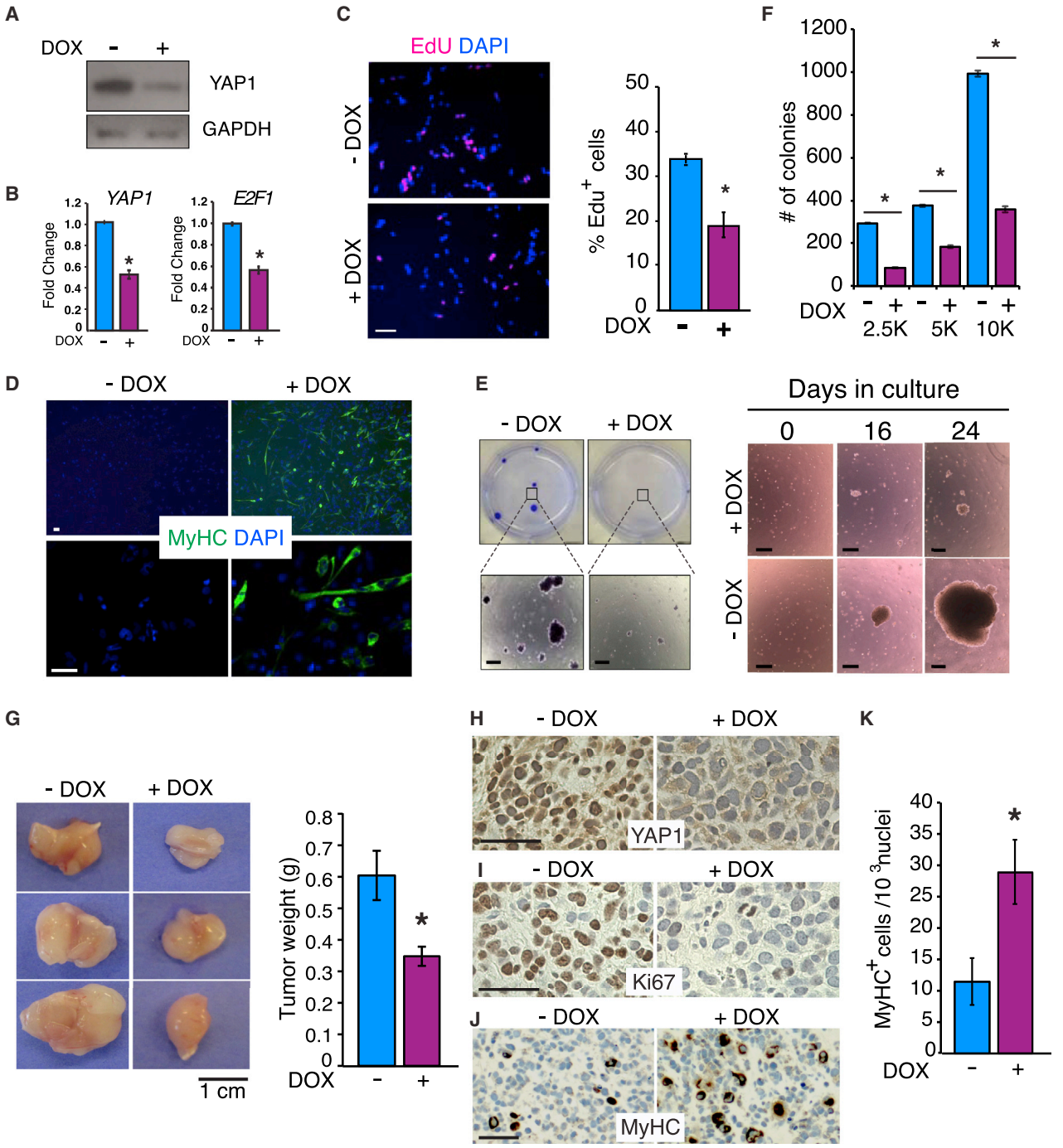

Figure 8. YAP1 Knockdown in ERMS Cells Decreases Tumor Burden and Rescues the ERMS Differentiation Block

(A) Western blot analysis of YAP1 levels in RD-TetO-shYAP1 cells, untreated and DOX treated for 5 days.

(B) *YAP1* and *E2F1* mRNA levels in DOX-treated RD-TetO-shYAP1 cells versus untreated cells.

(C) EdU incorporation in RD-TetO-shYAP1 cells in the presence and absence of DOX and quantification of EdU^+ cells (n = 3).

(D) Immunostaining for MyHC in RD-TetO-shYAP1 cells in the absence and presence of DOX in differentiation conditions.

(E) Soft agar colony formation assay of RD-TetO-shYAP1 in the presence and absence of DOX. Scale bars, 400 μm.

(F) Quantification of the number of colonies in soft agar colony formation assay as in (E), for increasing number of plated cells.

(G) Macroscopic picture of the xenograft tumors obtained from DOX-treated and untreated RD-TetO-shYAP1 cells and bar graph showing tumor weight at excision (n = 8 for DOX treated; n = 10 for untreated).

(H–J) Cross-sections of tumors in (G), immunostained for YAP1 (H), Ki67 (I), and MyHC (J). Scale bars, 50 μm.

(K) Quantification of MyHC staining as in (J).

All error bars are represented as ±SEM.

DISCUSSION

Here we show that YAP1 expression and activity are highest in human ERMS versus ARMS and find that many human ERMS, but not ARMS, harbor a copy number gain of the *YAP1* locus. In addition, high YAP1 activity is associated with poorer prognosis in human ERMS cases, but not in ARMS. Consistent with this, we show that high YAP1 activity causes ERMS-like tumors in mice with surprisingly short latency and high penetrance compared to other mouse models of RMS, identifying YAP1 as an exceptionally potent ERMS oncogene.

Using *Myf5*-, *Myod1*-, and *Pax7*-driven Cre alleles in combination with muscle injury, we identify activated, but not quiescent, satellite cells as the cell of origin of YAP1-driven ERMS. Overexpressing a constitutively active hYAP1 S127A mutant in other tissues such as liver (Camargo et al., 2007; Dong et al., 2007) and skin (Schlegelmilch et al., 2011) increases the proliferation of progenitors and organ size without the need for a concomitant activating signal or injury. This might represent inherent differences in the basal cycling activity of these tissues. Indeed, adult skeletal muscle has a low cellular turnover (Spalding et al., 2005) as satellite cells are normally mitotically quiescent and only rarely become activated to fulfill the sporadic demands for hypertrophy or repair. Intriguingly, this partly mirrors human pathogenesis as ERMS generally occurs in children and adolescents, where postnatal muscle growth is dependent on satellite cell activity (Parham and Ellison, 2006). Additionally, dystrophic mice, in which a large fraction of satellite cells is activated (Pallafacchina et al., 2010), spontaneously form RMS (Chamberlain et al., 2007; Hosur et al., 2012), and further studies are required to establish the role of aberrant YAP1 activity in muscular dystrophies and their associated RMS.

Although insufficient to activate quiescent satellite cells under homeostatic conditions in adult mice, YAP1 is sufficient to drive RMS from activated satellite cells by maintaining the myoblast state in a global manner. Indeed, YAP1 not only promotes persistent proliferation of activated satellite cells but also arguably acts as a meta-oncogene by promoting the expression of a number of oncogenes associated with RMS (*Myc*, *Met*, *Rras2*, *Maff*, *Birc5*/*Survivin*). In parallel, YAP1 also imposes a differentiation block in a direct and indirect manner via its transcriptional program.

First, YAP1-TEAD1 bind to the promoters of genes normally expressed only in terminally differentiated muscle and appear to repress the activity of myogenic factors by impinging on the recruitment of MYOD1 and MEF2 on myogenic differentiation-associated loci. While it was known since the late 1980s that a few differentiated skeletal muscle genes contain TEAD-targeted MCAT elements (Yoshida, 2008), our study demonstrates that YAP1-TEAD1 operate genome-wide to regulate lineage-specific gene expression in skeletal muscle. The repressive effect of YAP1-TEAD1 binding specifically on myogenic differentiation-associated loci also suggests that YAP1 is not only acting as a co-activator for the TEAD family of transcription factors. The transcriptional outcome of YAP1-TEAD1 binding most likely depends on the general chromatin context. Indeed, a repressive role of YAP1-TEAD1 was only reported recently in ES cells (Beyer et al., 2013), and taken together with our results, this supports the concept that YAP1-TEAD1 can be integrated into larger repressive complexes in a context- and lineage-specific manner. The notion that YAP1 can act with the same partner in multiple transcriptional mechanisms is intriguing, although in agreement with the different effects of YAP1 overexpression across various tissues (Barry et al., 2013; Camargo et al., 2007; Schlegelmilch et al., 2011).

Second, YAP1 also blocks the myogenic differentiation program in an indirect manner by upregulating the expression of known repressors of MYOD1 pro-differentiation activity (*Twist1*, *Mdfic*, *Snai1*, and *Snai2*). This is consistent with the idea that myogenic factors are expressed but inactive at completing the differentiation program in RMS and that the balance between MYOD1 activating or repressing heterodimers is shifted toward repression in RMS (Yang et al., 2009). Twist1 is a known repressive heterodimer partner of MYOD1 (Yang et al., 2009) and was previously reported to play a role in RMS development (Maestro et al., 1999). CABIN1 and MASTR are coregulators of MEF2 factors (Creemers et al., 2006; Jang et al., 2007; Meadows et al., 2008; Mokalled et al., 2012), and SNAI1 and SNAI2 were recently reported to direct MYOD1 away from its pro-differentiation targets genes in proliferating myoblasts (Soleimani et al., 2012). Thus, under high YAP1 activity, upregulation of TWIST1 and SNAI1 and SNAI2 expression by YAP1-TEAD1 likely adds another repressive layer for MYOD1 transcriptional activity on differentiation genes. Our study clearly demonstrates that the transcriptional program of YAP1-TEAD1 in ERMS can globally sustain the myoblast phenotype by acting simultaneously on several interlinked cellular functions including proliferation, transformation and terminal differentiation.

In addition, our study identifies YAP1 inhibition as a promising strategy for differentiation therapy of ERMS. Despite the recent report that the Hippo pathway, via its upstream regulator RASSF4, was involved in fusion-positive alveolar RMS (Crose et al., 2014), a direct link between ARMS development and YAP1 was not conclusively demonstrated. Our results might suggest a higher importance of YAP1 in ERMS development and propagation. Indeed, higher stage ERMS, which usually require more aggressive therapies, display elevated YAP1 activity and are associated with poorer prognosis, while the fusion positive tumors displaying high or low YAP1 activity appear equally aggressive. Reducing YAP1 activity in YAP1-ERMS tumors as well as in human ERMS RD cells was sufficient to decrease their proliferation and transformed state and resulted in myogenic differentiation. Importantly, we confirmed that differentiation therapy through YAP1 inhibition is effective not only in YAP1-driven mouse ERMS but also in more complex human ERMS tumors via orthotopic xenograft assays. Our results collectively support that YAP1 inhibition should be explored in preclinical studies as a differentiation therapy approach to restore differentiation of fusion-negative RMS in cooperation with other therapeutic modalities.

EXPERIMENTAL PROCEDURES

Mouse Strains, Animal Procedures, and Human Samples

The Pax7-cre/ERT2 (stock 012476), Myf5-Cre (stock 007893), Myod1-iCre (stock 014140), ZsGreen1 reporter (stock 007906), and NOD/SCID (stock 001303) mice were purchased from the Jackson Laboratory. The R26-Stop-rtTA and Col1a-TetO-hYAP1 S127A mice were previously described (Schlegelmilch et al., 2011). The Pax7-creERT2 mice were treated with tamoxifen (Sigma) solubilized in corn oil (Sigma) and administered as previously

described (Lepper and Fan, 2010). Doxycycline hyclate (Sigma) was administered in drinking water. Cardiotoxin from Naja naja mossambica (4.5 μM) (Sigma) was injected intra-muscularly 24 hr prior to transplantation (25 μl). All procedures were conducted in accordance with the Guidelines for the Care and Use of Laboratory Animals and were approved by the Boston Children's Hospital and Joslin Diabetes Center Institutional Animal Care and Use Committee. The human RMS sample collection from UK centers through the Children's Cancer and Leukemia Group was performed under the Local Research Ethics Committee protocol Nos. 1836 and 2015 and Multi-Regional Research Ethics Committee/06/4/71, with consent, as previously described (Tonelli et al., 2012; Wachtel et al., 2006).

Primary Cells Preparation, Stable Cell Line Generation, and Xenograft Assay

For transplantation in NOD/SCID hosts, muscle interstitial cells from DOX-induced donor mice (8 weeks induction) were prepared from a two-digest protocol as previously described (Sherwood et al., 2004). The tumors were dissociated using the same protocol except that a single combined digestion step was performed for 60–75 min at 37 degree. Cells were either transplanted into NOD/SCID hosts directly or sorted for expression of ZsGreen1 by flow cytometry as indicated. Sorted tumor cells were transplanted or cultured (Dulbecco's modified Eagle's medium supplemented with 20% fetal bovine serum, pen and strep, glutamine) in the presence of DOX (2 mg/mL). RD cells were infected with an inducible YAP1-TRIPz-TetO-shRNA lentivirus (Open Biosystems) expressing red fluorescent protein (RFP) and a short hairpin targeting *YAP1* upon DOX induction. Cells were selected with puromycin for 5 days, then DOX was added for an additional 4 days before RFP positive cells were sorted by flow cytometry. Sorted RD-TetO-shYAP1 cells were cultured for 4 days in the presence or absence of DOX, and then 4.4 million cells were transplanted into the GAS of injured NOD/SCID recipients.

Human RMS Tissue Microarray and Gene Expression Analysis

The human RMS tissue microarray construction and human samples collection were previously described (Tonelli et al., 2012; Wachtel et al., 2006). The gene expression profile of 235 RMS patients from two publicly available data sets were analyzed: one containing 101 samples [Innovative Therapies for Children with Cancer/Carte d'Identité des Tumeurs (ITCC/CIT)] (Williamson et al., 2010) and a second with 134 samples [Children's Oncology Group/Intergroup Rhabdomyosarcoma Study Group (COG/IRSG)] (Davicioni et al., 2009). Raw data for the COG/IRSG collection was obtained from the NCI Cancer Array Database and from Prof. M.J. Anderson. Raw data for the ITCC/CIT collection are in ArrayExpress (E-TABM-1202). The two data sets were normalized separately using a robust multiarray average. Gene expression profiles of normal skeletal muscles and other relevant controls were obtained from public resources; details are reported in the Supplemental Experimental Procedures.

ACCESSION NUMBERS

Microarray and ChIP-Seq data are deposited in the Gene Expression Omnibus database (GSE47198 and GSE55186, respectively).

SUPPLEMENTAL INFORMATION

Supplemental Information includes Supplemental Experimental Procedures, six figures, and three tables and can be found with this article online at http://dx.doi.org/10.1016/j.ccr.2014.05.029.

ACKNOWLEDGMENTS

We thank Kriti Shrestha for technical assistance. This research was funded by a Stand Up to Cancer-AACR initiative grant (F.D.C.), NIH grants AR064036 (F.D.C.) and DK099559 (F.D.C.), a Canadian Institutes of Health Research (CIHR) fellowship (A.M.T.), a Medical Research Council project grant (99477, H.W., P.S.Z., C.D.B.), an American-Italian Cancer Foundation postdoctoral research fellowship (G.G.G.), an Oliver Bird PhD studentship (R.J.), a Friends of Anchor pilot grant and a Sarcoma UK grant (H.W., G.M., C.D.B.), a Cancer Research UK project grant (C5066/A10399) (J.S.), a Chris Lucas Trust grant (J.S.), a Stand Up to Cancer-AACR Innovative Research Grant (SU2C-AACR-IRG1111) and NIH New Innovator Award (DP2 OD004345-01) (A.J.W.), and grants from P.A.L.S. Bermuda/St. Baldrick's and Alex's Lemonade Stand Foundation (S.H.). Mouse microarray studies were performed by the Molecular Genetics Core Facility at Children's Hospital Boston supported by NIH-P50-NS40828 and NIH-P30-HD18655. The Children's Cancer and Leukemia Group, and UK and NHS funding to the NIHR Biomedical Research Centre, assisted with human tissue collection. Confocal imaging was performed at the Children's Hospital Boston Imaging Core facility.

Received: May 14, 2013
Revised: April 8, 2014
Accepted: May 29, 2014
Published: July 31, 2014

REFERENCES

Al-Tahan, A., Sarkis, O., Harajly, M., Baghdadi, O.K., Zibara, K., Boulos, F., Dighe, D., Kregel, S., Bazarbachi, A., El-Sabban, M., et al. (2012). Retinoic acid fails to induce cell cycle arrest with myogenic differentiation in rhabdomyosarcoma. Pediatr. Blood Cancer *58*, 877–884.

Barry, E.R., Morikawa, T., Butler, B.L., Shrestha, K., de la Rosa, R., Yan, K.S., Fuchs, C.S., Magness, S.T., Smits, R., Ogino, S., et al. (2013). Restriction of intestinal stem cell expansion and the regenerative response by YAP. Nature *493*, 106–110.

Beauchamp, J.R., Heslop, L., Yu, D.S., Tajbakhsh, S., Kelly, R.G., Wernig, A., Buckingham, M.E., Partridge, T.A., and Zammit, P.S. (2000). Expression of CD34 and Myf5 defines the majority of quiescent adult skeletal muscle satellite cells. J. Cell Biol. *151*, 1221–1234.

Belyea, B., Kephart, J.G., Blum, J., Kirsch, D.G., and Linardic, C.M. (2012). Embryonic signaling pathways and rhabdomyosarcoma: contributions to cancer development and opportunities for therapeutic targeting. Sarcoma *2012*, 406239.

Beyer, T.A., Weiss, A., Khomchuk, Y., Huang, K., Ogunjimi, A.A., Varelas, X., and Wrana, J.L. (2013). Switch enhancers interpret TGF-β and Hippo signaling to control cell fate in human embryonic stem cells. Cell Reports *5*, 1611–1624.

Camargo, F.D., Gokhale, S., Johnnidis, J.B., Fu, D., Bell, G.W., Jaenisch, R., and Brummelkamp, T.R. (2007). YAP1 increases organ size and expands undifferentiated progenitor cells. Current biology: CB *17*, 2054–2060.

Chamberlain, J.S., Metzger, J., Reyes, M., Townsend, D., and Faulkner, J.A. (2007). Dystrophin-deficient mdx mice display a reduced life span and are susceptible to spontaneous rhabdomyosarcoma. FASEB journal: official publication of the Federation of American Societies for Experimental Biology *21*, 2195–2204.

Cornelison, D.D., and Wold, B.J. (1997). Single-cell analysis of regulatory gene expression in quiescent and activated mouse skeletal muscle satellite cells. Dev. Biol. *191*, 270–283.

Creemers, E.E., Sutherland, L.B., McAnally, J., Richardson, J.A., and Olson, E.N. (2006). Myocardin is a direct transcriptional target of Mef2, Tead and Foxo proteins during cardiovascular development. Development *133*, 4245–4256.

Crose, L.E., Galindo, K.A., Kephart, J.G., Chen, C., Fitamant, J., Bardeesy, N., Bentley, R.C., Galindo, R.L., Chi, J.T., and Linardic, C.M. (2014). Alveolar rhabdomyosarcoma-associated PAX3-FOXO1 promotes tumorigenesis via Hippo pathway suppression. J. Clin. Invest. *124*, 285–296.

Davicioni, E., Anderson, M.J., Finckenstein, F.G., Lynch, J.C., Qualman, S.J., Shimada, H., Schofield, D.E., Buckley, J.D., Meyer, W.H., Sorensen, P.H., and Triche, T.J. (2009). Molecular classification of rhabdomyosarcoma—genotypic and phenotypic determinants of diagnosis: a report from the Children's Oncology Group. Am. J. Pathol. *174*, 550–564.

Dong, J., Feldmann, G., Huang, J., Wu, S., Zhang, N., Comerford, S.A., Gayyed, M.F., Anders, R.A., Maitra, A., and Pan, D. (2007). Elucidation of a universal size-control mechanism in Drosophila and mammals. Cell *130*, 1120–1133.

Hatley, M.E., Tang, W., Garcia, M.R., Finkelstein, D., Millay, D.P., Liu, N., Graff, J., Galindo, R.L., and Olson, E.N. (2012). A mouse model of rhabdomyosarcoma originating from the adipocyte lineage. Cancer Cell *22*, 536–546.

Hosur, V., Kavirayani, A., Riefler, J., Carney, L.M., Lyons, B., Gott, B., Cox, G.A., and Shultz, L.D. (2012). Dystrophin and dysferlin double mutant mice: a novel model for rhabdomyosarcoma. Cancer Genet *205*, 232–241.

Jang, H., Choi, D.E., Kim, H., Cho, E.J., and Youn, H.D. (2007). Cabin1 represses MEF2 transcriptional activity by association with a methyltransferase, SUV39H1. J. Biol. Chem. *282*, 11172–11179.

Judson, R.N., Tremblay, A.M., Knopp, P., White, R.B., Urcia, R., De Bari, C., Zammit, P.S., Camargo, F.D., and Wackerhage, H. (2012). The Hippo pathway member Yap plays a key role in influencing fate decisions in muscle satellite cells. J. Cell Sci. *125*, 6009–6019.

Judson, R.N., Gray, S.R., Walker, C., Carroll, A.M., Itzstein, C., Lionikas, A., Zammit, P.S., De Bari, C., and Wackerhage, H. (2013). Constitutive expression of Yes-associated protein (Yap) in adult skeletal muscle fibres induces muscle atrophy and myopathy. PLoS ONE *8*, e59622.

Kanisicak, O., Mendez, J.J., Yamamoto, S., Yamamoto, M., and Goldhamer, D.J. (2009). Progenitors of skeletal muscle satellite cells express the muscle determination gene, MyoD. Dev. Biol. *332*, 131–141.

Keller, C., Arenkiel, B.R., Coffin, C.M., El-Bardeesy, N., DePinho, R.A., and Capecchi, M.R. (2004). Alveolar rhabdomyosarcomas in conditional Pax3:Fkhr mice: cooperativity of Ink4a/ARF and Trp53 loss of function. Genes Dev. *18*, 2614–2626.

Kuang, S., Kuroda, K., Le Grand, F., and Rudnicki, M.A. (2007). Asymmetric self-renewal and commitment of satellite stem cells in muscle. Cell *129*, 999–1010.

Lepper, C., and Fan, C.M. (2010). Inducible lineage tracing of Pax7-descendant cells reveals embryonic origin of adult satellite cells. Genesis *48*, 424–436.

Lian, I., Kim, J., Okazawa, H., Zhao, J., Zhao, B., Yu, J., Chinnaiyan, A., Israel, M.A., Goldstein, L.S., Abujarour, R., et al. (2010). The role of YAP transcription coactivator in regulating stem cell self-renewal and differentiation. Genes Dev. *24*, 1106–1118.

Maestro, R., Dei Tos, A.P., Hamamori, Y., Krasnokutsky, S., Sartorelli, V., Kedes, L., Doglioni, C., Beach, D.H., and Hannon, G.J. (1999). Twist is a potential oncogene that inhibits apoptosis. Genes Dev. *13*, 2207–2217.

Meadows, S.M., Warkman, A.S., Salanga, M.C., Small, E.M., and Krieg, P.A. (2008). The myocardin-related transcription factor, MASTR, cooperates with MyoD to activate skeletal muscle gene expression. Proc. Natl. Acad. Sci. USA *105*, 1545–1550.

Missiaglia, E., Williamson, D., Chisholm, J., Wirapati, P., Pierron, G., Petel, F., Concordet, J.P., Thway, K., Oberlin, O., Pritchard-Jones, K., et al. (2012). PAX3/FOXO1 fusion gene status is the key prognostic molecular marker in rhabdomyosarcoma and significantly improves current risk stratification. J. Clin. Oncol. *30*, 1670–1677.

Mokalled, M.H., Johnson, A.N., Creemers, E.E., and Olson, E.N. (2012). MASTR directs MyoD-dependent satellite cell differentiation during skeletal muscle regeneration. Genes Dev. *26*, 190–202.

Pallafacchina, G., François, S., Regnault, B., Czarny, B., Dive, V., Cumano, A., Montarras, D., and Buckingham, M. (2010). An adult tissue-specific stem cell in its niche: a gene profiling analysis of in vivo quiescent and activated muscle satellite cells. Stem Cell Res. (Amst.) *4*, 77–91.

Parham, D.M., and Ellison, D.A. (2006). Rhabdomyosarcomas in adults and children: an update. Arch. Pathol. Lab. Med. *130*, 1454–1465.

Rossi, S., Poliani, P.L., Cominelli, M., Bozzato, A., Vescovi, R., Monti, E., and Fanzani, A. (2011). Caveolin 1 is a marker of poor differentiation in Rhabdomyosarcoma. Eur. J. Cancer *47*, 761–772.

Rubin, B.P., Nishijo, K., Chen, H.I., Yi, X., Schuetze, D.P., Pal, R., Prajapati, S.I., Abraham, J., Arenkiel, B.R., Chen, Q.R., et al. (2011). Evidence for an unanticipated relationship between undifferentiated pleomorphic sarcoma and embryonal rhabdomyosarcoma. Cancer Cell *19*, 177–191.

Saab, R., Spunt, S.L., and Skapek, S.X. (2011). Myogenesis and rhabdomyosarcoma the Jekyll and Hyde of skeletal muscle. Curr. Top. Dev. Biol. *94*, 197–234.

Schlegelmilch, K., Mohseni, M., Kirak, O., Pruszak, J., Rodriguez, J.R., Zhou, D., Kreger, B.T., Vasioukhin, V., Avruch, J., Brummelkamp, T.R., and Camargo, F.D. (2011). Yap1 acts downstream of α-catenin to control epidermal proliferation. Cell *144*, 782–795.

Seale, P., Bjork, B., Yang, W., Kajimura, S., Chin, S., Kuang, S., Scimè, A., Devarakonda, S., Conroe, H.M., Erdjument-Bromage, H., et al. (2008). PRDM16 controls a brown fat/skeletal muscle switch. Nature *454*, 961–967.

Sherwood, R.I., Christensen, J.L., Conboy, I.M., Conboy, M.J., Rando, T.A., Weissman, I.L., and Wagers, A.J. (2004). Isolation of adult mouse myogenic progenitors: functional heterogeneity of cells within and engrafting skeletal muscle. Cell *119*, 543–554.

Soleimani, V.D., Yin, H., Jahani-Asl, A., Ming, H., Kockx, C.E., van Ijcken, W.F., Grosveld, F., and Rudnicki, M.A. (2012). Snail regulates MyoD binding-site occupancy to direct enhancer switching and differentiation-specific transcription in myogenesis. Mol. Cell *47*, 457–468.

Spalding, K.L., Bhardwaj, R.D., Buchholz, B.A., Druid, H., and Frisén, J. (2005). Retrospective birth dating of cells in humans. Cell *122*, 133–143.

Tajbakhsh, S., Bober, E., Babinet, C., Pournin, S., Arnold, H., and Buckingham, M. (1996). Gene targeting the myf-5 locus with nlacZ reveals expression of this myogenic factor in mature skeletal muscle fibres as well as early embryonic muscle. Dev. Dyn. *206*, 291–300.

Tiffin, N., Williams, R.D., Shipley, J., and Pritchard-Jones, K. (2003). PAX7 expression in embryonal rhabdomyosarcoma suggests an origin in muscle satellite cells. Br. J. Cancer *89*, 327–332.

Tonelli, R., McIntyre, A., Camerin, C., Walters, Z.S., Di Leo, K., Selfe, J., Purgato, S., Missiaglia, E., Tortori, A., Renshaw, et al.. (2012). Antitumor activity of sustained N-myc reduction in rhabdomyosarcomas and transcriptional block by antigene therapy. Clin. Cancer Res. *18*, 796–807.

Tremblay, A.M., and Camargo, F.D. (2012). Hippo signaling in mammalian stem cells. Semin. Cell Dev. Biol. *23*, 818–826.

Wachtel, M., Runge, T., Leuschner, I., Stegmaier, S., Koscielniak, E., Treuner, J., Odermatt, B., Behnke, S., Niggli, F.K., and Schafer, B.W. (2006). Subtype and prognostic classification of rhabdomyosarcoma by immunohistochemistry. J. Clin. Oncol. *24*, 816–822.

Watt, K.I., Judson, R., Medlow, P., Reid, K., Kurth, T.B., Burniston, J.G., Ratkevicius, A., De Bari, C., and Wackerhage, H. (2010). Yap is a novel regulator of C2C12 myogenesis. Biochem. Biophys. Res. Commun. *393*, 619–624.

Williamson, D., Missiaglia, E., de Reyniès, A., Pierron, G., Thuille, B., Palenzuela, G., Thway, K., Orbach, D., Laé, M., Fréneaux, P., et al. (2010). Fusion gene-negative alveolar rhabdomyosarcoma is clinically and molecularly indistinguishable from embryonal rhabdomyosarcoma. J. Clin. Oncol. *28*, 2151–2158.

Yang, Z., MacQuarrie, K.L., Analau, E., Tyler, A.E., Dilworth, F.J., Cao, Y., Diede, S.J., and Tapscott, S.J. (2009). MyoD and E-protein heterodimers switch rhabdomyosarcoma cells from an arrested myoblast phase to a differentiated state. Genes Dev. *23*, 694–707.

Yoshida, T. (2008). MCAT elements and the TEF-1 family of transcription factors in muscle development and disease. Arterioscler. Thromb. Vasc. Biol. *28*, 8–17.

Yu, F.X., and Guan, K.L. (2013). The Hippo pathway: regulators and regulations. Genes Dev. *27*, 355–371.

Zhao, B., Wei, X., Li, W., Udan, R.S., Yang, Q., Kim, J., Xie, J., Ikenoue, T., Yu, J., Li, L., et al. (2007). Inactivation of YAP oncoprotein by the Hippo pathway is involved in cell contact inhibition and tissue growth control. Genes Dev. *21*, 2747–2761.

Zhao, B., Ye, X., Yu, J., Li, L., Li, W., Li, S., Yu, J., Lin, J.D., Wang, C.Y., Chinnaiyan, A.M., et al. (2008). TEAD mediates YAP-dependent gene induction and growth control. Genes Dev. *22*, 1962–1971.

Zhou, D., Zhang, Y., Wu, H., Barry, E., Yin, Y., Lawrence, E., Dawson, D., Willis, J.E., Markowitz, S.D., Camargo, F.D., and Avruch, J. (2011). Mst1 and Mst2 protein kinases restrain intestinal stem cell proliferation and colonic tumorigenesis by inhibition of Yes-associated protein (Yap) overabundance. Proc. Natl. Acad. Sci. USA *108*, E1312–E1320.